Recent armed conflict disrupts atmospheric climate monitoring

Sebastian Scher* Florian Ladstädter

Wegener Center for Climate and Global Change, University of Graz, Graz, Austria

Both authors contributed equally *Corresponding author: sebastian.scher@uni-graz.at

September 2026

Preprint notice. This manuscript is a non-peer-reviewed preprint submitted to EarthArXiv. It has not undergone formal peer review and may be revised in response to community feedback or during subsequent journal review. Please cite the corresponding EarthArXiv version when referring to this work. The manuscript is currently under review at Environmental Research Letters.

Abstract. The unprecedented use of GPS jamming in the Russo-Ukrainian war severely disrupts GNSS Radio Occultation, a key remote sensing technique for climate monitoring and weather forecasting. Since 2018, a growing systematic gap in atmospheric observations has extended far beyond the direct conflict zone. This loss of data substantially impairs atmospheric temperature monitoring, introducing observation errors large enough to bias climate trend estimates.

Keywords: Climate monitoring, Radio Occultation, Remote Sensing, GPS Jamming

1 Introduction

Recent armed conflicts, particularly the Russo-Ukrainian war, have triggered unprecedented, large-scale disruption of Global Navigation Satellite Systems (GNSS) for navigation and communication, through deliberate interference commonly referred to as GPS jamming [1, 2]. GNSS Radio Occultation (RO)—a satellite remote sensing technique with uniquely high vertical resolution, all-weather capability, and exceptional long-term stability with minimal instrumental drift—has become a cornerstone of atmospheric climate monitoring and numerical weather prediction [3–6]. Because RO relies directly on GNSS signals as its core measurement, it is inherently vulnerable to GPS jamming [7]. Disruption of GNSS signals degrades the signal-to-noise ratio in RO retrievals and reduces the number of profiles that can be successfully obtained, leading to a substantial reduction in observation density. This loss of RO data is not merely a technical side effect of GNSS jamming, but constitutes a direct and potentially serious threat to our ability to monitor the climate system. Here, we provide the first systematic assessment of how GPS jamming degrades RO observations and compromises atmospheric temperature monitoring, with direct implications for the quality of climate data records, weather forecasting, and reanalysis datasets [8].

2 Decrease in observations

The impact of GPS jamming on RO observations is manifested in a clearly visible gap in profile coverage centered over eastern Ukraine and western Russia for the widely used Metop-B satellite [9] in the most recent 12-month period (Fig. 1a), compared with the situation before 2018. This gap is consistently observed across other global RO missions (Fig. S1).

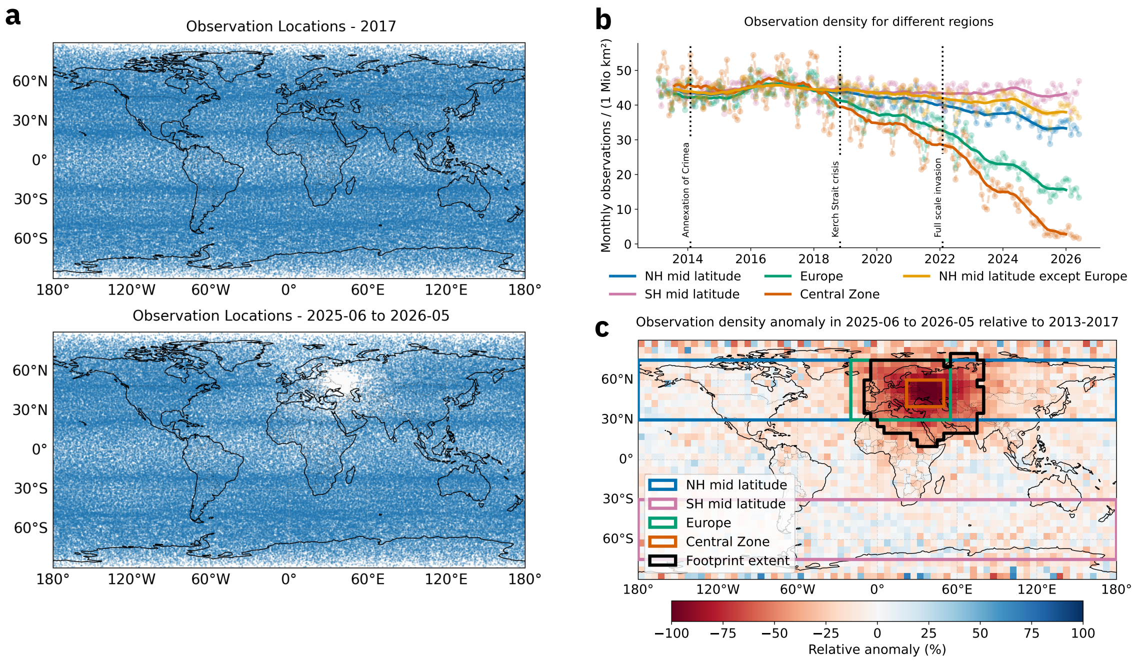

Figure 1: Regional decline in atmospheric observations over time. a, Individual Metop-B GNSS radio occultation observations in 2017 (upper panel) and the most recent 12-month period June 2025 to May 2026 (lower panel), showing a pronounced gap centred over eastern Ukraine and western Russia. **b**, Normalized monthly observation density from January 2013 to May 2026 for five geographical regions. Dots show monthly values and solid lines 12-month running means. The black dotted lines indicate several major events in the Russo-Ukrainian war. **c**, Relative change in observation density in June 2025–May 2026 compared with the 2013–2017 baseline. The black contour outlines the region where observation density decreased by at least 35%.

Before 2018, RO observation densities from Metop-B were comparable across different regions, at roughly 45 observations per million square kilometres per month. Starting in early 2018, however, observation densities within the central zone around eastern Ukraine and western Russia decline steadily, reaching only about 3 observations per million square kilometres per month by 2025—a reduction of more than 90% (Fig. 1b, regions shown in Fig. 1c).

The timeline is consistent with reports of increased use of GPS jamming in the Russo-Ukrainian war [1, 2]. A substantial, though smaller, decline is also evident across the broader European region, where densities drop to approximately 18 observations per million square kilometres per month, a reduction of about 40%. Across the Northern Hemisphere mid-latitudes, the observation density drops to approximately 35 observations per million square kilometres per month. In contrast, Southern Hemisphere mid-latitudes show no significant change, clearly demonstrating that the decline is not attributable to orbital effects, satellite receiver or retrieval issues, but to regional GPS jamming.

We objectively identify the region of reduced observations by computing observation-density anomalies relative to the mean density during the Metop-B period preceding the decline (2013 to 2017). During the most recent 12-month period, a distinct region over eastern Ukraine and western Russia exhibits a decrease of nearly 100%, indicating a complete lack of observations (Fig. 1c), surrounded by a much larger region with a smaller, but still substantial, reduction in observation density. The black line in Fig. 1c outlines connected grid points with a decrease of at least 35%. This region extends far beyond the conflict zone, from the Iberian Peninsula and the British Isles in the west to the northeastern parts of South Asia in the east, and from North Africa in the south to Scandinavia in the north, clearly showing that RO observations are negatively affected far beyond the central conflict zone. This region of reduced observation density has developed gradually since 2018 (see Fig. S2, which shows the relative observation density anomaly for all other years).

3 Impact on climate monitoring

Such a large, contiguous region of reduced observation density—and, in its center, a complete absence of observations—potentially has a significant detrimental effect on climate monitoring. We assess how the loss in local observations affects the atmospheric monitoring capabilities of RO. For this, we quantify the impact of the observation loss seen in the most recent 12-month period by applying the current sampling pattern to an earlier, unaffected reference period. Using data from before 2018, we randomly remove observations within the objectively identified affected region until local observation densities match those observed in the recent 12-month interval. The differences between these reduced datasets and the original, full sampling provide an estimate of the errors introduced by the reduction in observations.

There is a central region of around $15° \times 15°$, centered over eastern Ukraine and western Russia, where the atmosphere is completely unobserved by RO. It is surrounded by a region where the reduction in observations leads to monthly mean temperature errors up to 4 K in the free atmosphere, with errors gradually declining with increasing distance from the central zone (Fig. 2a). These errors are large enough to affect zonal means between $25°\,\mathrm{N}$ and $75°\,\mathrm{N}$, with the largest errors between $50°\,\mathrm{N}$ and $60°\,\mathrm{N}$ reaching up to 0.35 K (Fig. 2b). The zonal mean error has a relevant systematic component, with missing observations introducing a warm bias of up to 0.25 K (Fig. 2c), which can reach 1 K in certain months and varies considerably over individual years (Fig. 2d). This temporal variability implies that simple bias correction methods are insufficient to correct for the errors.

Finally, we assess how the gradual increase in missing observations since 2018 has affected atmospheric temperature trend estimates, which have so far not explicitly accounted for the substantial regional decline in observational coverage (e.g., [10]). From 2018 onward, in addition to random errors, there is an increasing systematic bias with strong interannual variability (Fig. 2e); particularly in winter, the growing number of missing observations leads to an increasing warm bias in observed temperatures. This bias causes altitude-dependent errors in temperature trend estimates from -0.07 K per

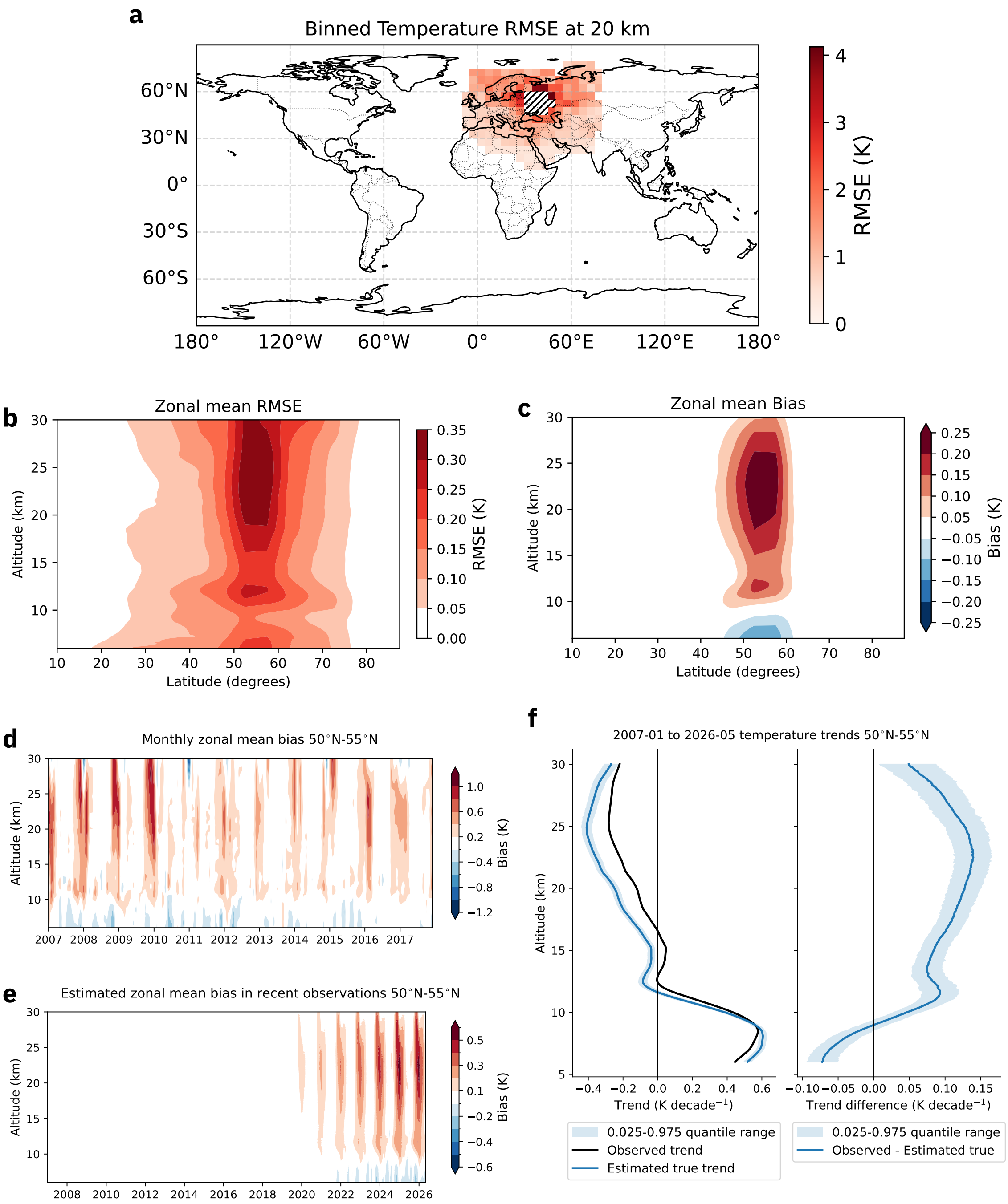

Figure 2: Impact of missing observations on climate monitoring. a, Root-mean-square error (RMSE) in temperature at 20 km altitude, estimated retrospectively for 2013 to 2017 under a sampling scenario in which observations are missing as in June 2025 to May 2026. Hatching indicates regions with such a reduction in observations that they are effectively unobserved. **b**, RMSE in zonal-mean temperature estimated using the same sampling scenario as in **a**. **c**, Bias in zonal-mean temperature estimated using the same sampling scenario as in **a**. **d**, Bias in zonal-mean temperature for individual months, estimated using the sampling scenario in **a**. **e**, Estimated bias in observed monthly-mean temperature for January 2007 to May 2026 due to missing observations. **f**, Zonal temperature trends from estimated true and observed records for January 2007 to May 2026, shown alongside the difference between the two trends.

decade at 6 km altitude to over $+0.13$ K per decade at higher altitudes for the centrally affected latitude band $50° \mathrm{N}$ to $55° \mathrm{N}$ (Fig. 2f). These trend errors are only about a factor of 2 to 3 smaller than the actual observed trends (-0.2 to $+0.6$ K per decade, depending on altitude) and are therefore large enough to substantially affect inferred temperature trends. Zonal-mean temperature trends from RO data are likely underestimated from 2018 onward at most altitudes, by up to 60% around 25 km.

4 Discussion

We used a zonal mean definition that is inherently more robust to local gaps by first averaging individual RO profiles into $5° \times 5°$ (latitude $\times$ longitude) bins and then averaging these bin means. Averaging over $5° \times 10°$ bins yields similar results (Fig. S3). In contrast, directly averaging all RO profiles within a latitude band—a simple but widely used method—the errors become considerably larger (RMSE up to 1.4 K, bias over 1 K, monthly errors over 3 K), and the trend even changes sign at altitudes above 12 km (Fig. S4), substantially misrepresentating atmospheric temperature trends. This demonstrates that careful consideration on which method to use is required when computing zonal means for latitudes affected by GPS jamming, an issue that is normally minor for RO data due to its near-zonal homogeneity in observation locations. Nevertheless, even with more robust bin-averaging approaches, a significant bias remains. A central issues identified here is that missing observations introduce a systematic bias whose magnitude increases over time. While trend estimates are robust to constant systematic biases, a gradually increasing bias inevitably introduces a systematic error into the trend estimates.

5 Implications and outlook

Our results show that GPS jamming surrounding the Russo-Ukrainian war has reached a level that significantly disrupts our capability to observe the atmosphere. A region over eastern Ukraine and western Russia has become essentially unobservable with GNSS RO, with substantially reduced observation density extending far beyond the central jamming region. The resulting errors in atmospheric temperature observations are large enough to persist even when averaging over entire zonal bands. The consequences are substantial errors in monthly means and multi-decade climate trends, both essential for climate monitoring and climate model evaluation. A critical review of RO-based climate data and estimated trends is therefore necessary to correct for errors introduced by the regional decrease in observations.

In our analysis, we quantified the impact of GPS jamming on GNSS RO, an atmospheric remote sensing technique that is particularly sensitive to disruptions of GNSS signals. However, GNSS interference may also affect other atmospheric observing systems, such as modern radiosondes, highlighting the need for observation techniques that are robust against GPS jamming and other disruptions to ensure accurate long-term atmospheric climate monitoring and reliable weather prediction. On a wider scale, our results show that armed conflicts and wars—in addition to causing human suffering and economic losses— are significantly disrupting environmental monitoring in previously unanticipated ways.

In light of these findings, policy makers and funding agencies responsible for the planning and sustainability of Earth observation systems should recognize GPS jamming and GNSS interference as a *systemic risk* to the global climate observing infrastructure. Long-term strategies for satellite mission design, ground-based observing networks, and data assimilation systems must explicitly account for the possibility of regional or persistent GNSS denial. This includes (i) investing in technological redundancy, such as multi-GNSS capable receivers, alternative positioning and timing systems, and complementary observing techniques that are less sensitive to GNSS interference; (ii) supporting robust reprocessing and correction frameworks capable of identifying and mitigating jamming-induced biases in climate data records; and (iii) developing international norms and agreements that recognize the critical societal role of uninterrupted environmental monitoring, even in times of conflict. Proactive planning and targeted funding in these areas are essential to safeguard the integrity of atmospheric and climate observations, maintain reliable inputs for numerical weather prediction and climate models, and ensure that global climate monitoring remains resilient in a geopolitically unstable world.

Data availability

Data sources and availability are explained in detail in the supplementary material.

Acknowledgements

We thank Andrea Steiner and Matthias Stocker for their valuable input on data sources, visualization and framing, Marc Schwärz for discussions on RO missions and retrieval, and Mariya Donska for advice on language related to geopolitical issues.

References

[1] Nereida Rodriguez-Alvarez, Xavier Bosch-Lluis, and Kamal Oudrhiri. A Decade of GNSS Signal Disruptions in SMAP-R Full-Polarimetric Observations Worldwide. *IEEE J. Sel. Top. Appl. Earth Obs. Remote Sens.*, 19:4228–4241, 2026. ISSN 2151-1535. doi: 10.1109/JSTARS.2026.3652089.

[2] Zachary L. Clements, Argyris Kriezis, and Todd E. Humphreys. Chasing Lightning: Detecting, Characterizing, and Identifying a Powerful Space-Based GNSS Interference Source, June 2026.

[3] Emil Robert Kursinski, George A. Hajj, J. Tim Schofield, Roger P. Linfield, and Kenneth R. Hardy. Observing Earth's atmosphere with radio occultation measurements using the Global Positioning System. *J. Geophys. Res.*, 102(D19):23429–23465, 1997. doi: 10.1029/97JD01569.

[4] L. Cucurull, R. A. Anthes, and L.-L. Tsao. Radio Occultation Observations as Anchor Observations in Numerical Weather Prediction Models and Associated Reduction of Bias Corrections in Microwave and Infrared Satellite Observations. *J. Atmos. Oceanic Technol.*, 31(1):20–32, 2014. doi: 10.1175/JTECH-D-13-00059.1.

[5] Andrea Karin Steiner, Florian Ladstädter, William J. Randel, Amanda C. Maycock,

Qiang Fu, Chantal Claud, Hans Gleisner, Leopold Haimberger, Shu-Peng Ho, Philippe Keckhut, Thierry Leblanc, Carl Mears, Lorenzo M. Polvani, Benjamin D. Santer, Torsten Schmidt, Viktoria F. Sofieva, Robin Wing, and Cheng-Zhi Zou. Observed Temperature Changes in the Troposphere and Stratosphere from 1979 to 2018. *J. Climate*, 33 (19):8165–8194, 2020. doi: 10.1175/JCLI-D-19-0998.1.

[6] Hui Shao, Ulrich Foelsche, Anthony J. Mannucci, Irfan Azeem, Neill E. Bowler, John J. Braun, Katrin Lonitz, Christian Marquardt, Andrea K. Steiner, Benjamin Ruston, and Panagiotis Vergados. Advances in GNSS-Based Remote Sensing for Weather, Climate, and Space Weather: Missions, Applications, and Emerging Techniques. *Bull. Amer. Meteor. Soc.*, 106(7):E1471–E1477, July 2025. ISSN 0003-0007, 1520-0477. doi: 10.1175/BAMS-D-25-0138.1.

[7] Dong L. Wu. GNSS Signal Jamming as Observed From Radio Occultation. *IEEE J. Sel. Top. Appl. Earth Obs. Remote Sens.*, 17:8642–8645, 2024. ISSN 2151-1535. doi: 10.1109/JSTARS.2024.3385738.

[8] Paul Poli, Sean B. Healy, and Dick P. Dee. Assimilation of global positioning system radio occultation data in the ECMWF ERA-Interim reanalysis. *Q. J. R. Meteor. Soc.*, 136(653):1972–1990, 2010. doi: 10.1002/qj.722.

[9] Kenneth Holmlund, Paul Counet, Fran Martinez Fadrique, Alexander Schmid, Bojan Bojkov, Rosemary Munro, Jochen Grandell, and Estelle Obligis. The EUMETSAT satellite programmes and data services. *J. Eur. Meteorol. Soc.*, 2:100005, June 2025. ISSN 2950-6301. doi: 10.1016/j.jemets.2024.100005. URL https://www.sciencedirect.com/science/article/pii/S295063012400005X.

[10] Florian Ladstädter, Andrea K. Steiner, and Hans Gleisner. Resolving the 21st century temperature trends of the upper troposphere–lower stratosphere with satellite observations. *Sci. Rep.*, 13(1306), 2023. doi: 10.1038/s41598-023-28222-x.

Supplementary Information for "Recent armed conflict disrupts atmospheric climate monitoring"

Sebastian Scher*	Florian Ladstädter

Wegener Center for Climate and Global Change, University of Graz, Graz, Austria

Both authors contributed equally	*Corresponding author: sebastian.scher@uni-graz.at

September 2026

Contents

1 Supplementary figures **2**

2 Data and methods **6**

2.1 GNSS Radio Occultation 6
2.2 Data 6
2.3 Zonal means 6
2.4 Climate trends 6
2.5 Estimating the impact of missing observations 7
2.5.1 Impact on monthly means 7
2.5.2 Impact on observed trends 7

1 Supplementary figures

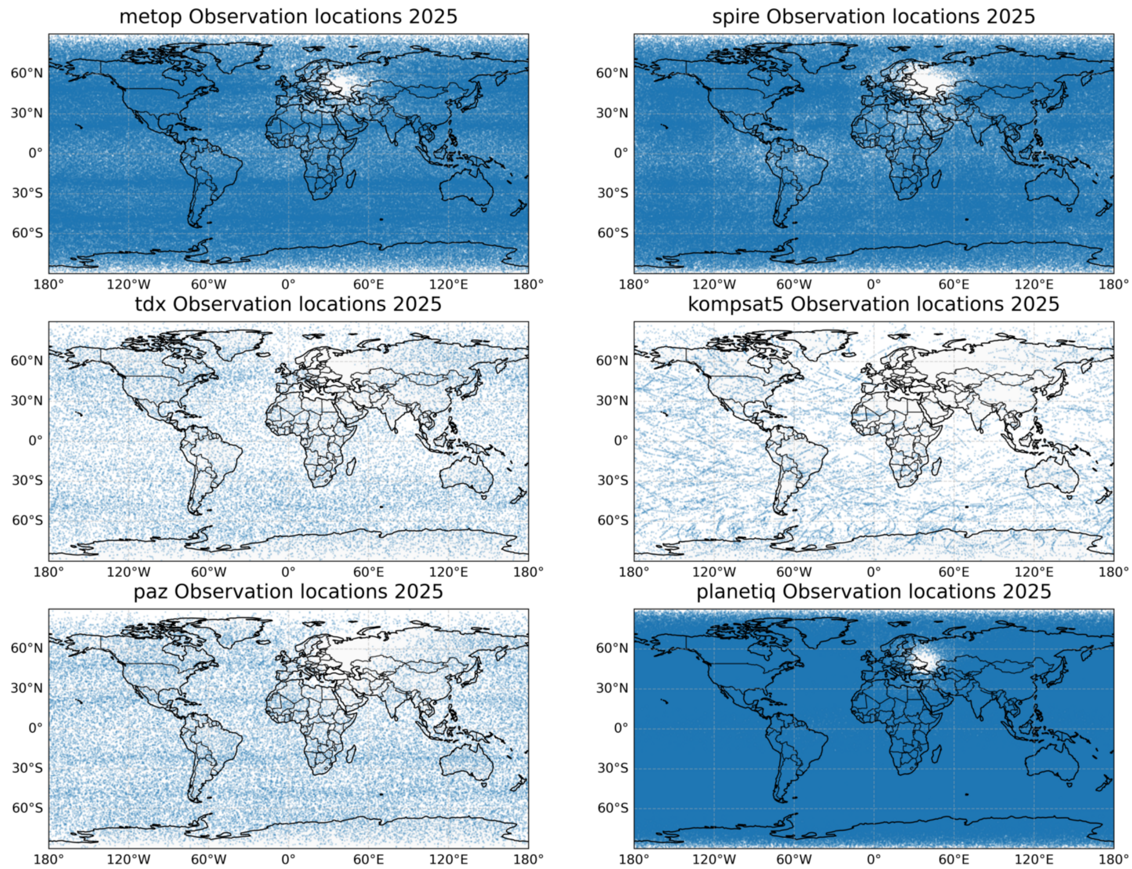

Figure 1: Observations from different RO missions for 2025: Metop-A and Metop-B combined (metop), Spire, TanDEM-X (tdx), Kompsat5, PAZ and PlanetiQ

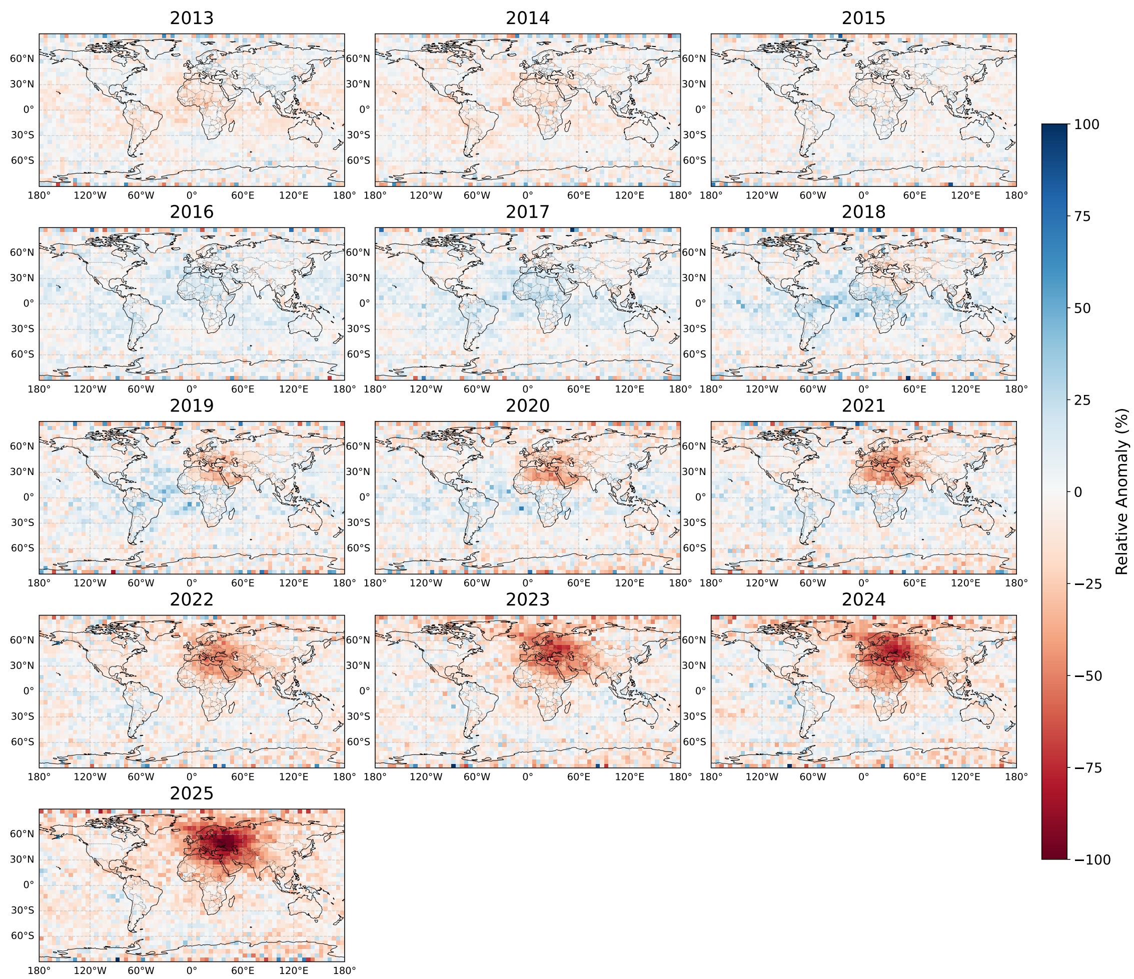

Figure 2: Relative change in observation density for each year from 2013 to 2025 compared with the 2013–2017 baseline.

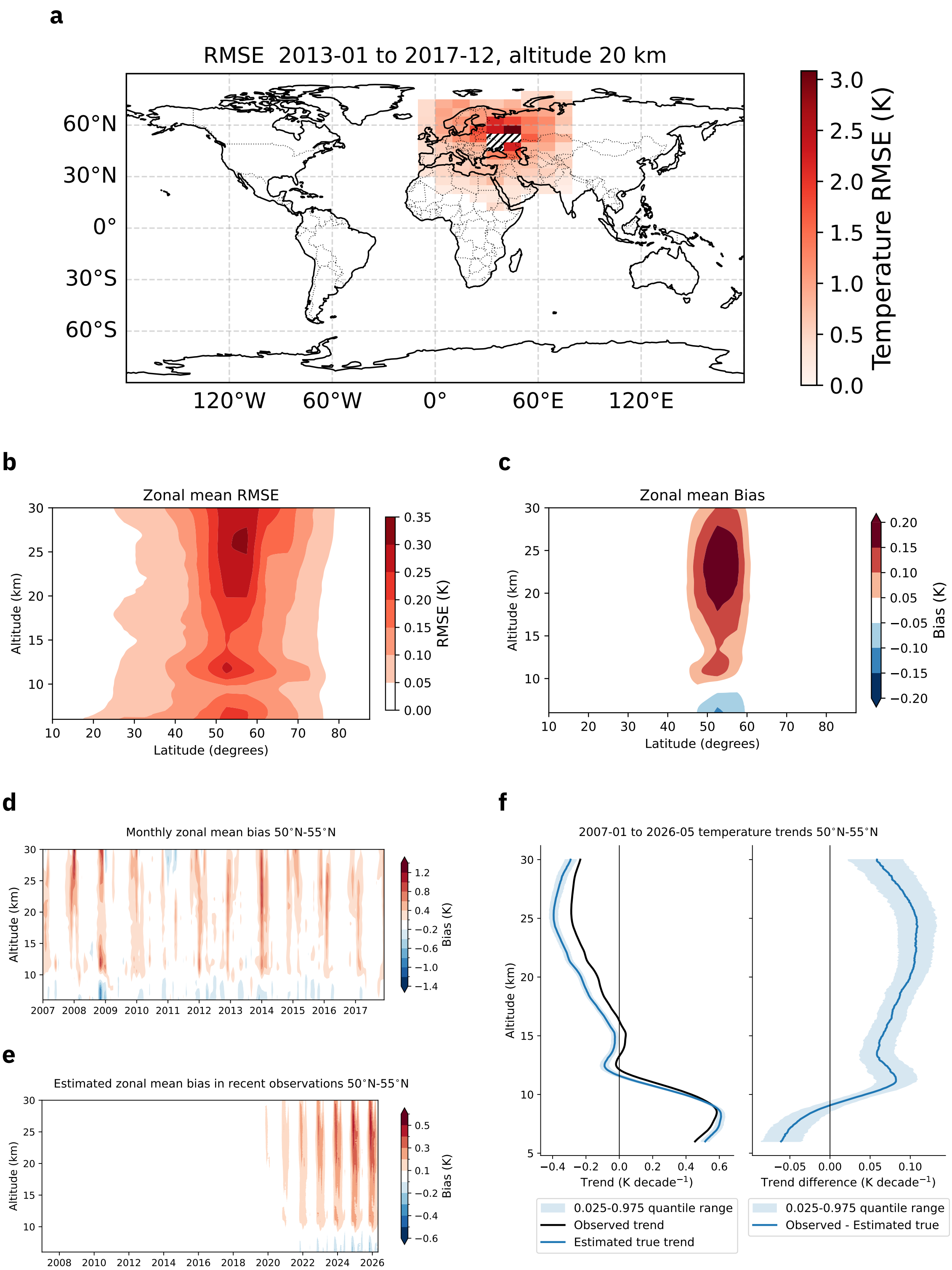

Figure 3: Impact of missing observations on climate monitoring with 5x10 binning. a, Root-mean-square error (RMSE) in temperature at 20 km altitude, estimated retrospectively for 2013 to 2017 under a sampling scenario in which observations are missing as in June 2025 to May 2026. Hatching indicates regions with such a reduction in observations that they are effectively unobserved. **b**, RMSE in zonal-mean temperature estimated using the same sampling scenario as in **a**. **c**, Bias in zonal-mean temperature estimated using the same sampling scenario as in **a**. **d**, Bias in zonal-mean temperature for individual months, estimated using the sampling scenario in **a**. **e**, Estimated bias in observed monthly-mean temperature for January 2007 to May 2026 due to missing observations. **f**, Zonal temperature trends from estimated true and observed records for January 2007 to May 2026, shown alongside the difference between the two trends.

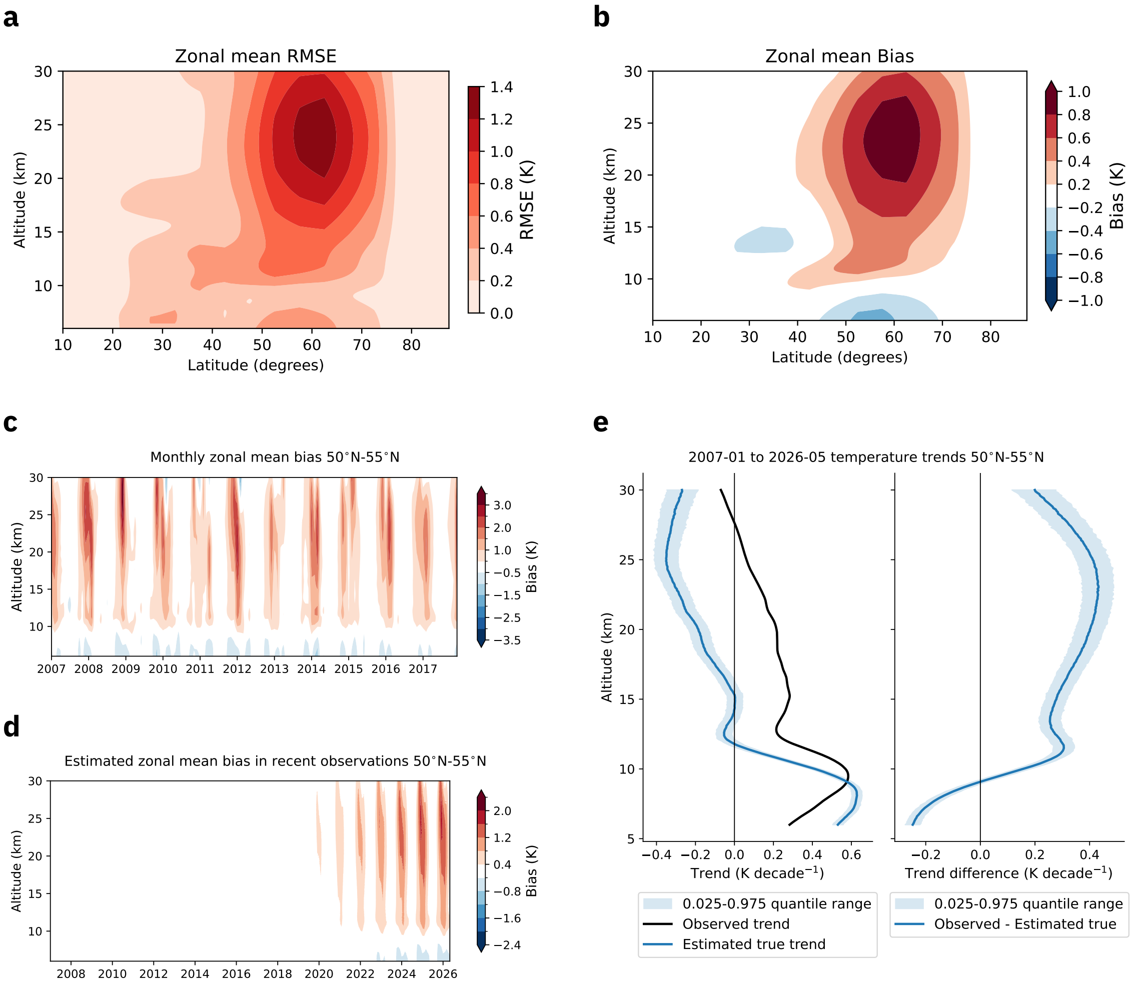

Figure 4: Impact of missing observations on climate monitoring with zonal mean computed by averaging all observations in a latitude band in a given month. a, Root-mean-square error (RMSE) in temperature at 20 km altitude, estimated retrospectively for 2013 to 2017 under a sampling scenario in which observations are missing as in June 2025 to May 2026. Hatching indicates regions with such a reduction in observations that they are effectively unobserved. **b**, RMSE in zonal-mean temperature estimated using the same sampling scenario as in **a**. **c**, Bias in zonal-mean temperature estimated using the same sampling scenario as in **a**. **d**, Bias in zonal-mean temperature for individual months, estimated using the sampling scenario in **a**. **e**, Estimated bias in observed monthly-mean temperature for January 2007 to May 2026 due to missing observations. **f**, Zonal temperature trends from estimated true and observed records for January 2007 to May 2026, shown alongside the difference between the two trends.

2 Data and methods

2.1 GNSS Radio Occultation

GNSS RO uses electromagnetic signals transmitted by GNSS satellites, including GPS, and received by satellites in low Earth orbit. Combined with precise orbit information, the measured signal phase is used to retrieve atmospheric bending and refractivity, from which temperature and pressure profiles are derived [1].

The orbital characteristics of the transmitting and receiving satellite constellations result in measurements that are distributed quasi-randomly in space and time. Their global coverage, high vertical resolution, all-weather capability and long-term stability make GNSS RO observations particularly valuable for resolving atmospheric structure and detecting long-term climate change [2].

2.2 Data

The GNSS profiles were retrieved from the Radio Occultation Meteorology Satellite Application Facility (ROM SAF) [3]. Observations were obtained from the Meteorological Operational satellite programme (Metop), specifically Metop-A, Metop-B and Metop-C, which form the space segment of the EUMETSAT Polar System (EPS) [4]. Metop-B is the only satellite providing a largely constant number of globally distributed RO observations for several years both before and after the onset of the disruptions in 2018. Using a single satellite allows to objectively identify a baseline observation density. Therefore, all results in Fig. 1 are estimated exclusively from Metop-B data.

To estimate the biases introduced by missing observations, it is crucial to use RO data in the way it would normally be used in long-term climate monitoring. The default approach is to combine multiple RO satellites [5, 6]. Therefore, the results in Fig. 2 are based on a combined time series of all three Metop satellites (Metop-A, Metop-B and Metop-C), as provided by ROM SAF.

For visualizing observations of other RO missions (Fig. S1), profile metadata for the missions Spire, TanDEM-X, Kompsat5, PAZ and PlanetiQ were obtained from the AWS Open Data Registry [7]. Due to the limited availability of processed data for 2026, this visualization was based on 2025.

2.3 Zonal means

Zonal monthly means are computed in three different ways: (1) by first computing monthly means within $5^\circ \times 5^\circ$ bins and then averaging over those bins; (2) by computing monthly means within $5^\circ \times 10^\circ$ bins and then averaging over those bins; and (3) by averaging all profiles within a 5° latitude band for the given month.

2.4 Climate trends

Climate trends are computed on all Metop missions for January 2007 to May 2026, with least square linear regressions on monthly anomalies. Monthly anomalies are computed with respect to the mean for each month of the year over the full period January 2007 to May 2026.

2.5 Estimating the impact of missing observations

2.5.1 Impact on monthly means

The impact of missing observations on monthly gridded means and monthly zonal means is estimated retrospectively using data from before 2018 (i.e., before the onset of disruptions). To this end, an artificially reduced RO dataset is constructed. In each $5^\circ \times 5^\circ$ degrees grid box, RO observations are randomly removed according to the observation density anomalies shown in Fig. 1c. An anomaly of -100% corresponds to a 100% probability of removal. Monthly means are then computed for both the original and the artificially reduced dataset. The difference between these two monthly means provides an estimate of the error that the reduction in observation density during the period June 2025 to May 2026 has on RO-based monthly mean grid boxes and on the zonal means computed from them. Due to the definition of the affected region shown in Fig. 1c, by construction the impact is zero outside this region.

2.5.2 Impact on observed trends

The impact of missing observations on observed atmospheric temperature trends is estimated using Monte Carlo simulations. Based on the results for the impact on monthly means computed for the unaffected period before 2018, we infer the impact on the affected period from 2018 to 2026. We assume that the errors estimated using data before 2018 are representative of the actual errors that occur from 2018 onwards.

The errors before 2018 were estimated for the observation reduction observed in the most recent available 12-month period, June 2025 to May 2026. For each month of the year, we compute the mean bias and the standard deviation of the bias over the artificially reduced data for 2007 to 2017. We assume that these mean and standard deviation estimates are representative of the observation reduction observed during June 2025 to May 2026.

Based on the results shown in Fig. 1b, we further assume that the errors are zero in 2018 and increase linearly to their full values in 2025. To implement this, we linearly scale both the mean and the standard deviation of the errors. For each month in the period 2018 to 2025, we take the mean and standard deviation of the errors corresponding to that month of the year, apply the linear scaling, and draw a random value from the distribution. This error is then subtracted from the actually observed value for that month. The procedure is applied separately to each zonal band. The entire process is repeated 10,000 times, yielding 10,000 time series that represent possible realizations of the true atmospheric temperatures.

Temporal climate trends are then computed over the period January 2007 to May 2026 for each of the 10,000 time series, as well as for the uncorrected observed time series. The blue shading in Fig. 2f denotes the spread of the Monte Carlo simulations. The spread of the trends across the 10,000 realizations quantifies the uncertainty in climate trends induced by missing RO observations in the affected region. Note that, by construction, the period before 2018 is unaffected by this procedure, as we assume it is not influenced by any reduction in observations.

References

[1] Emil Robert Kursinski, George A. Hajj, J. Tim Schofield, Roger P. Linfield, and Kenneth R. Hardy. Observing Earth's atmosphere with radio occultation measurements using the Global Positioning System. *J. Geophys. Res.*, 102(D19):23429–23465, 1997. doi: 10.1029/97JD01569.

[2] Andrea Karin Steiner, Florian Ladstädter, William J. Randel, Amanda C. Maycock, Qiang Fu, Chantal Claud, Hans Gleisner, Leopold Haimberger, Shu-Peng Ho, Philippe Keckhut, Thierry Leblanc, Carl Mears, Lorenzo M. Polvani, Benjamin D. Santer, Torsten Schmidt, Viktoria F. Sofieva, Robin Wing, and Cheng-Zhi Zou. Observed Temperature Changes in the Troposphere and Stratosphere from 1979 to 2018. *J. Climate*, 33(19): 8165–8194, 2020. doi: 10.1175/JCLI-D-19-0998.1.

[3] ROM SAF. ROM SAF Climate data record v1.0 and v1.1, 2021. URL https://rom-saf.eumetsat.int/.

[4] Kenneth Holmlund, Paul Counet, Fran Martinez Fadrique, Alexander Schmid, Bojan Bojkov, Rosemary Munro, Jochen Grandell, and Estelle Obligis. The EUMETSAT satellite programmes and data services. *J. Eur. Meteorol. Soc.*, 2:100005, June 2025. ISSN 2950-6301. doi: 10.1016/j.jemets.2024.100005. URL https://www.sciencedirect.com/science/article/pii/S295063012400005X.

[5] Andrea Karin Steiner, Florian Ladstädter, Chi O. Ao, Hans Gleisner, Shu-Peng Ho, Douglas Hunt, Torsten Schmidt, Ulrich Foelsche, Gottfried Kirchengast, Ying-Hwa Kuo, Kent B. Lauritsen, Anthony J. Mannucci, Johannes K. Nielsen, William Schreiner, Marc Schwärz, Sergey Sokolovskiy, Stig Syndergaard, and Jens Wickert. Consistency and structural uncertainty of multi-mission GPS radio occultation records. *Atmos. Meas. Tech.*, 13(5):2547–2575, 2020. doi: 10.5194/amt-13-2547-2020.

[6] Hans Gleisner, Mark A. Ringer, and Sean B. Healy. Monitoring global climate change using GNSS radio occultation. *NPJ Clim. Atmos. Sci.*, 5, 2022. doi: 10.1038/s41612-022-00229-7.

[7] S. S. Leroy, A. E. McVey, S. M. Leidner, H. Zhang, and H. Gleisner. GNSS radio occultation data in the AWS cloud. *Earth Space Sci.*, 11(2):e2023EA003021, 2024. doi: https://doi.org/10.1029/2023EA003021.